Drought stress delays photosynthetic induction and accelerates photoinhibition of photosystem I under fluctuating light

Hu Sun[1,2], Qi Shi[1,2], Ning-Yu Liu[1,2], Shi-Bao Zhang[1], Wei Huang[1]

[1] Kunming Institute of Botany, Chinese Academy of Sciences, Kunming 650201, China

[2] University of Chinese Academy of Sciences, Beijing 100049, China

Corresponding authors:

Shi-Bao Zhang: sbzhang@mail.kib.ac.cn

Wei Huang: huangwei@mail.kib.ac.cn

Funding:

1. the National Natural Science Foundation of China (No. 31971412, 32171505).

2. the Project for Innovation Team of Yunnan Province.

Running head:

Photosynthesis under drought and fluctuating light

Abstract

Fluctuating light (FL) and drought stress usually occur concomitantly. However, whether drought stress affects photosynthetic performance under FL remains unknown. Here, we measured gas exchange, chlorophyll fluorescence, and P700 redox state under FL in drought-stressed tomato (*Solanum lycopersicum*) seedlings. Drought stress significantly affected stomatal opening and mesophyll conductance after transition from low to high light and thus delayed photosynthetic induction under FL. Therefore, drought stress exacerbated the loss of carbon gain under FL. Furthermore, restriction of CO_2 fixation under drought stress aggravated the over-reduction of photosystem I (PSI) upon transition from low to high light. The resulting stronger FL-induced PSI photoinhibition significantly supressed linear electron flow and PSI photoprotection. These results indicated that drought stress not only affected gas exchange under FL but also accelerated FL-induced photoinhibition of PSI. Furthermore, drought stress enhanced relative cyclic electron flow in FL, which partially compensated for restricted CO_2 fixation and thus favored PSI photoprotection under FL. Therefore, drought stress has large effects on photosynthetic dark and light reactions under FL.

Keywords: drought, fluctuating light, photoinhibition, photosynthesis, stomatal conductance, tomato.

Acknowledgements:

The authors acknowledge the financial support by the National Natural Science Foundation of China (No. 31971412, 32171505) and the Project for Innovation Team of Yunnan Province.

Conflict of Interest:

The authors declare no conflict of interest.

Introduction

During diurnal photosynthesis under natural field conditions, leaves usually experience dynamic changes in light intensity on timescales from milliseconds to hours, owing to the variation of the solar angle, cloud movement, wind-induced leaf fluttering, and shading from overlapping leaves and neighboring plants (Pearcy 1990; Slattery, Walker, Weber & Ort 2018). In addition to fluctuating light (FL), plants often experience suboptimal conditions, such as drought. Many studies have examined the effect of drought stress on photosynthesis under stable light intensity (Oukarroum, Schansker & Strasser 2009; Galmés *et al.* 2013; Zivcak *et al.* 2013). However, drought stress is rarely studied under FL conditions (Grieco *et al.* 2020; Qu *et al.* 2020). Under FL, plants may exhibit different photosynthetic performance when also experiencing drought stress compared with sufficient water conditions. To understand how plants perform under a combination of FL and drought stress in the field, it is important to explore the photosynthetic physiology of drought-stressed plants under FL.

After transition from low to high light, the net CO_2 assimilation rate (A_N) gradually increases, which is termed “photosynthetic induction”. The rate of photosynthetic induction significantly affects carbon gain and thus affects plant biomass when grown under FL (Adachi *et al.* 2019; Kimura, Hashimoto-Sugimoto, Iba, Terashima & Yamori 2020; Yamori, Kusumi, Iba & Terashima 2020). Therefore, promoting the rate of photosynthetic induction is a potential target for improving crop yield (De Souza, Wang, Orr, Carmo-Silva & Long 2020; Acevedo-Siaca *et al.* 2020). Under high light, A_N is determined by CO_2 diffusional conductance and biochemical factors (Grassi & Magnani 2005). CO_2 diffusional conductance refers to CO_2 diffusion from the atmosphere to the chloroplast stroma, including stomatal conductance (g_s) and mesophyll conductance (g_m) (Flexas *et al.* 2014). Biochemical factors include the activation of electron transport, Calvin–Benson cycle enzymes, especially Rubisco, and sucrose synthesis (Sakoda, Yamori, Groszmann & Evans 2021). A recent study revealed that the induction of A_N under FL was mainly affected by g_s rather than g_m in *Arabidopsis thaliana* and tobacco (*Nicotiana tabacum*) plants in the absence of water stress (Sakoda *et al.* 2021). Increasing the stomatal opening significantly enhanced the induction of A_N and plant biomass under FL (Kimura *et al.* 2020; Yamori *et al.* 2020). Drought stress

usually reduces g_s and g_m under constant high light, leading to decreased chloroplast CO_2 concentration (C_c) (Warren, Livingston & Turpin 2004). Under such conditions, CO_2 fixation in chloroplast carboxylation sites is restricted by the lack of CO_2. Therefore, the relative limitations of g_s and g_m imposed on A_N are enhanced under drought stress. However, it is unclear whether drought stress affects the induction responses of g_s, g_m, and A_N under FL. Characterizing the dynamics of g_s and g_m and how they limit A_N under drought and FL is crucial for understanding the physiological mechanisms regulating carbon gain by plants under suboptimal field conditions.

In addition to photosynthetic dark reactions, FL affects photosynthetic light reactions. Upon a sudden increase in light intensity, electron flow from photosystem II (PSII) to photosystem I (PSI) rapidly increases (Huang, Yang & Zhang 2019a; Sun, Zhang, Liu & Huang 2020b). Meanwhile, CO_2 fixation is not fully activated (Tanaka, Adachi & Yamori 2019), generating an imbalance between the production of excited states and the consumption of reducing power (Gerotto *et al.* 2016; Tan, Huang, Zhang, Zhang & Huang 2021). The resulting PSI over-reduction increases the production of reactive oxygen species (ROS) in PSI. Consequently, oxidative damage to PSI occurs because the ROS produced within thylakoid membranes cannot be immediately scavenged by antioxidant systems (Takagi, Takumi, Hashiguchi, Sejima & Miyake 2016). Therefore, FL can cause selective photoinhibition of PSI in many angiosperms (Yamori, Makino & Shikanai 2016; Yamamoto & Shikanai 2019; Huang, Yang & Zhang 2019b). PSI damage suppresses photosynthetic electron flow, photoprotection, and CO_2 assimilation (Sejima, Takagi, Fukayama, Makino & Miyake 2014; Zivcak, Brestic, Kunderlikova, Sytar & Allakhverdiev 2015; Shimakawa & Miyake 2019), first impairing plant growth and even causing plant death (Suorsa *et al.* 2012; Yamori *et al.* 2016). The PSI redox state under FL is significantly affected by the electron sink downstream of PSI (Wada *et al.* 2018; Tazoe *et al.* 2020; Sun, Yang & Huang 2020a). However, little is known about the effects of drought stress on the PSI redox state and PSI photoinhibition under FL.

Plants have evolved several alternative electron flows to protect PSI against photoinhibition under FL (Allahverdiyeva, Suorsa, Tikkanen & Aro 2015; Armbruster, Correa Galvis, Kunz & Strand 2017; Shikanai & Yamamoto 2017). Cyclic electron flow (CEF)

around PSI is used by angiosperms to fine-turn photosynthetic apparatus under FL (Suorsa *et al.* 2012; Yamamoto & Shikanai 2019). After transition from low to high light, CEF activity usually increases to allow fast formation of the trans-thylakoid proton gradient (ΔpH), which alleviates the PSI over-reduction at donor and acceptor sides (Kono, Noguchi & Terashima 2014; Yang, Ding & Huang 2019a). Once a sufficient ΔpH forms, CEF activity decreases to steady-state levels to prevent over-acidification of the thylakoid lumen. Therefore, the dynamic regulation of CEF activity under FL is crucial for balancing photoprotection and photosynthesis (Alboresi, Storti & Morosinotto 2019). Previous studies have documented that CEF activity under FL is largely affected by the redox state of PSI (Yang *et al.* 2019a; Tan *et al.* 2021). In particular, CEF activity increases with moderate PSI over-reduction but maintains at a low level when PSI over-reduction is missing. However, the effects of drought stress on the dynamic regulation of CEF activity under FL is largely unknown.

The aim of this study was to investigate whether and how drought stress affects photosynthetic light and dark reactions under FL. With this knowledge it may be possible to understand how drought stress interacts with FL to affect photosynthetic physiology and plant growth. Tomato was used in this study, as it is a C3 model species with intermediate leaf photosynthetic capacity and an important vegetable crop worldwide. To address the above question, tomato plants were grown under full sun light with sufficient or deficient water. We then measured the rapid changes in gas exchange, chlorophyll fluorescence, and P700 signals under FL.

Materials and methods

Plant materials and growth conditions

Tomato (*Solanum lycopersicum* Miller cv. Hupishizi) plants were grown in a greenhouse under 40% full sunlight. Day/night air temperatures were approximately 30/20ºC, relative humidity was approximately 60-70%, and maximum light intensity was approximately 800 μmol photons m^{-2} s^{-1}. The plants were grown in 19-cm diameter plastic pots with humus soil, and the initial soil N content was 2.1 mg/g. Plants were fertilized with 0.15 g N/plant every two days using Peters Professional's water solution (N:P:K = 15:4.8:24.1) and watered every day. After cultivation for one and a half months, plants were watered using running water with

400g/pot (CK) or 200g/pot (drought) for 1 week, and then mature leaves were used for photosynthetic measurements.

Chlorophyll content measurement in vivo

A handheld chlorophyll meter (SPAD-502 Plus; Minolta, Tokyo, Japan) was used to non-destructively measure the relative content of chlorophyll per unit leaf area.

Gas exchange and chlorophyll fluorescence measurements

An open gas exchange system (LI-6400XT; Li-Cor Biosciences, Lincoln, NE, USA) was used to simultaneously measure gas exchange and chlorophyll fluorescence. After photosynthetic induction at 1500 μmol photons m^{-2} s^{-1} and 400 μmol mol^{-1} CO_2 concentration for 20 min, the net CO_2 assimilation rate and g_s reached steady-state values. Then, the light intensity was changed to 100 μmol photons m^{-2} s^{-1} for 5 min to conduct low light adaptation. Afterward, the light intensity was changed back to 1500 μmol photons m^{-2} s^{-1} to measure the photosynthetic induction phase. After adequate photosynthetic induction, the response of CO_2 assimilation rate to incident intercellular CO_2 concentration (A/C_i) curves were measured by decreasing the CO_2 concentration to a lower limit of 50 μmol mol^{-1} and then increasing stepwise to an upper limit of 1500 μmol mol^{-1}. For each CO_2 concentration, photosynthetic measurement was completed in 3 min. Using the A/C_i curves, the maximum rates of RuBP regeneration (J_{max}) and carboxylation (V_{cmax}) were calculated (Long & Bernacchi 2003).

The quantum yield of PSII photochemistry was calculated as $\Phi_{PSII} = (F_m' - F_s)/F_m'$ (Genty, Briantais & Baker 1989), where F_m' and F_s represent the maximum and steady-state fluorescence after light adaptation, respectively (Baker 2004). The total electron transport rate through PSII (J_{PSII}) was calculated as follows (Krall & Edwards 1992):

$$J_{PSII} = \Phi_{PSII} \times PPFD \times L_{abs} \times 0.5$$

where PPFD is the photosynthetic photon flux density and leaf absorbance (L_{abs}) is assumed to be 0.84. We applied the constant of 0.5 based on the assumption that photons were equally distributed between PSI and PSII.

Estimation of mesophyll conductance and chloroplast CO_2 concentration

Mesophyll conductance was calculated according to the following equation (Harley, Loreto, Di Marco & Sharkey 1992):

$$g_m = \frac{A_N}{C_i - \Gamma^*(J_{PSII} + 8(A_N + R_d))/(J_{PSII} - 4(A_N + R_d))}$$

where A_N represents the net rate of CO_2 assimilation; C_i is the intercellular CO_2 concentration; Γ^* is the CO_2 compensation point in the absence of daytime respiration (Yamori, Noguchi, Hikosaka & Terashima 2010b; von Caemmerer & Evans 2015), and we used a typical value of 40 μmol mol^{-1} in our current study (Xiong, Douthe & Flexas 2018). Respiration rate in the dark (R_d) was considered to be half of the dark-adapted mitochondrial respiration rate as measured after 10 min of dark adaptation (Carriquí *et al.* 2015).

Based on the estimated g_m, we then calculated the chloroplast CO_2 concentration (C_c) according to the following equation (Long & Bernacchi 2003; Warren & Dreyer 2006):

$$C_c = C_i - \frac{A_N}{g_m}$$

To identify the rate-limiting step of CO_2 assimilation, we subsequently estimated C_{trans} (the chloroplast CO_2 concentration at which the limitation to A_N transitioned from RuBP carboxylation to RuBP regeneration) (Yamori, Evans & Von Caemmerer 2010a; Yamori, Nagai & Makino 2011):

$$C_{trans} = \frac{K_c(1 + O/K_o)J_{max}/4V_{cmax} - 2\Gamma^*}{1 - J_{max}/4V_{cmax}}$$

where K_c (μmol mol^{-1}) and K_o (mmol mol^{-1}) are assumed to be 407 μmol mol^{-1} and 277 mmol mol^{-1} at 25ºC, respectively (Long and Bernacchi 2003); O was assumed to be 210 mmol mol^{-1} (Farquhar et al. 1980). The rate-limiting step for CO_2 assimilation was analyzed by comparing the values of C_c and C_{trans}. A_N tends to be limited by RuBP carboxylation when C_c is lower than C_{trans} and tends to be limited by RuBP regeneration when C_c is higher than C_{trans}.

Quantitative limitation analysis of A_N

Relative photosynthetic limitations were assessed as follows (Grassi & Magnani 2005):

$$L_s = \frac{g_{tot}/g_s \times \partial A_N/\partial C_c}{g_{tot} + \partial A_N/\partial C_c}$$

$$L_{mc} = \frac{g_{tot}/g_m \times \partial A_N/\partial C_c}{g_{tot} + \partial A_N/\partial C_c}$$

$$L_b = \frac{g_{tot}}{g_{tot} + \partial A_N / \partial C_c}$$

where L_s, L_{mc}, and L_b represent the relative limitations of stomatal conductance, mesophyll conductance, and biochemical capacity, respectively, in setting the observed value of A_N. g_{tot} is the total conductance of CO_2 between the leaf surface and sites of RuBP carboxylation (calculated as $1/g_{tot} = 1/g_s + 1/g_m$).

P700 and chlorophyll fluorescence measurements

PSI and PSII parameters were measured at 25ºC under atmospheric CO_2 condition using a Dual-PAM 100 measuring system (Heinz Walz, Effeltrich, Germany). Light from a 635-nm light-emitting diode array equipped in Dual-PAM 100 was used as actinic light for illumination. After dark adaptation for at least 15 min, a saturating pulse (20,000 μmol photons m^{-2} s^{-1}, 300 ms) was used to measure the maximum fluorescence intensity (F_m) and the maximum photo-oxidizable P700 (P_m). Subsequently, leaves were exposed to 1455 μmol photons m^{-2} s^{-1} for 5 min to activate photosynthetic electron sinks and then illuminated at fluctuating light alternating between low light (59 μmol photons m^{-2} s^{-1}, 2 min) and high light (1455 μmol photons m^{-2} s^{-1}, 1 min). During this fluctuating light treatment, PSI and PSII parameters were recorded simultaneously. After the fluctuating light treatment, P_m was measured after a 15-min dark adaptation.

The chlorophyll fluorescence parameters were calculated as follows: Y(II) = (F_m' − F_s)/ F_m'; NPQ = (F_m − F_m')/ F_m'; Y(NO) = F_s/F_m. Y(II) is the quantum yield of PSII photochemistry; NPQ, non-photochemical quenching in PSII; Y(NO), the quantum yield of non-regulatory energy dissipation in PSII. F_m and F_m' are the maximum fluorescence intensity after dark and light acclimation, respectively. F_s is the light-adapted steady-state fluorescence.

PSI photosynthetic parameters were measured by a Dual PAM-100 based on P700 signal (difference of intensities of 830 and 875 nm pulse-modulated measuring light reaching the photodetector). The $P700^+$ signals (P) may vary between a minimal (P700 fully reduced) and a maximal level (P700 fully oxidized). The maximum level (P_m) was determined with application of a saturating pulse (20,000 μmol photons m^{-2} s^{-1} and 300 ms) after pre-illumination with far-red light, and P_m was used to estimate the PSI activity. P_m' was

determined similarly to P_m but with actinic light instead of far-red light. PSI parameters were calculated as follows: Y(I) = (P_m' − P)/P_m; Y(ND) = P/P_m; Y(NA) = (P_m − P_m')/P_m. Y(I) is the quantum yield of PSI photochemistry; Y(ND), the quantum yield of PSI non-photochemical energy dissipation due to donor side limitation; Y(NA), the quantum yield of PSI non-photochemical energy dissipation due to acceptor side limitation. The photosynthetic electron transport rate was calculated as ETRI (or ETRII) = PPFD × Y(I) [or Y(II)] × 0.84 × 0.5, light absorption is assumed to be 0.84 of incident irradiance, and 0.5 is the fraction of absorbed light reaching PSI or PSII. The relative CEF value was measured by the ratio of Y(I) to Y(II) (Grieco *et al.* 2020).

Statistical analysis

One-way ANOVA and t-tests were used to determine whether significant differences existed between different treatments (α = 0.05). The software SigmaPlot 10.0 was used for graphing and fitting.

Results

Effects of drought stress on gas exchange under FL

After water deficit treatment for one week, the maximum quantum yield of PSII after dark adaptation was maintained at approximately 0.84 (data not shown), indicating that PSII activity was not significantly photoinhibited under drought stress. At low light intensity of 100 μmol photons m^{-2} s^{-1}, the steady-state net rate of CO_2 assimilation (A_N) was slightly affected by drought stress. However, drought stress significantly affected steady-state A_N, stomatal conductance (g_s), and mesophyll conductance (g_m) under high light. Furthermore, the photosynthetic induction after transition from low to high light was largely affected by drought stress (Fig. 1A). After transition from 100 to 1500 μmol photons m^{-2} s^{-1} for 1 min, A_N rapidly increased to 17.5 μmol m^{-2} s^{-1} in control (CK) plants but only increased to 4.0 μmol m^{-2} s^{-1} under drought (Fig. 1A). The time required for A_N to reach 80% of the maximum value was approximately 2 min in CK plants but 10 min under drought stress (Fig. 1B). Drought stress decreased g_s under low and high light compared to CK levels (Fig. 1C). Furthermore, the g_s level at low light was greatly reduced under drought stress compared with

the maximum g_s under high light, whereas there was less relative difference in g_s between low and high light in CK (Fig. 1D). Drought stress also lowered g_m under high light compared to CK (Fig. 1E). After transition from 100 to 1500 μmol photons m^{-2} s^{-1}, the time taken for g_m to reach the maximum value was approximately 3 min in CK plants but 11 min under drought stress (Fig. 1F). Therefore, drought stress delayed the induction responses of g_s, g_m, and A_N under FL.

Due to lower levels of CO_2 diffusional conductance, the intercellular CO_2 concentration (C_i) and chloroplast CO_2 concentration (C_c) under high light largely decreased under drought stress compared to CK (Fig. 2A and B). The values of C_c during photosynthetic induction were always higher than C_{trans} (the chloroplast CO_2 concentration at which the limitation to A_N transitioned from RuBP carboxylation to RuBP regeneration) in CK plants but were always lower than C_{trans} under drought stress, indicating that A_N tended to be limited by RuBP regeneration in CK plants and by RuBP carboxylation under drought stress. Therefore, the rate-limiting step for A_N during photosynthetic induction was altered by drought stress. The change in A_N during photosynthetic induction was tightly and positively correlated to C_c (Fig. 2C), indicating CO_2 fixation under FL was largely restricted by C_c. Quantitative analysis of photosynthetic limitations revealed stomatal limitation (L_s) and mesophyll conductance limitation (L_{mc}) were enhanced under drought stress (Fig. 3A and B). Concomitantly, biochemistry limitation (L_b) decreased under drought stress (Fig. 3C). Therefore, the major limitation of photosynthesis under FL also changed under drought stress.

Effects of drought stress on light reactions under FL

During photosynthetic induction, the quantum yield of PSI photochemistry (Y(I)) under high-light phases decreased under drought stress (Fig. 4A), whereas the PSI donor side limitation (Y(ND)) decreased under drought stress (Fig. 4B), leading to the higher PSI acceptor side limitation (Y(NA)) in plants exposed to drought stress (Fig. 4C). Therefore, drought stress induced stronger PSI over-reduction under FL. Furthermore, under sufficient water supply, the PSI over-reduction under FL was mainly observed after transitioning from low to high light for 10 s (Fig. 4C). By comparison, plants also displayed severe PSI over-reduction after this light transition for 30 s under drought stress (Fig. 4C). Therefore,

drought stress prolonged the time course of PSI over-reduction under FL.

Similar to Y(I), drought stress decreased the value of Y(II) at high light during photosynthetic induction (Fig. 5A). The induction response of NPQ was not affected by drought stress (Fig. 5B), leading to small changes in the quantum yield of non-regulatory energy dissipation in PSII (Y(NO)) between CK and drought-stressed plants (Fig. 5C). Drought stress had minimal effects on electron transport rates through PSI and PSII (ETRI and ETRII) at low light (Fig. 6A and B). However, the relative values of ETRI and ETRII under high light significantly decreased after drought treatment (Fig. 6A and B), which was consistent with the decreased A_N under drought stress. The relative CEF value under high light, measured as the ratio of Y(I) to Y(II), was higher in drought-stressed plants compared to CK plants (Fig. 6C). Furthermore, CEF could not be fully activated within the first 10 s under drought stress, suggesting that drought stress induced a delayed activation of CEF under FL. Therefore, the changing model of CEF under FL was altered by drought stress.

After FL treatment, the decrease in P_m was significantly higher under drought stress (Fig. 7A), indicating that drought stress significantly accelerated PSI photoinhibition under FL. The greater FL-induced PSI photoinhibition under drought stress was largely caused by the stronger PSI over-reduction within the first 30 s after transition from low to high light (Fig. 7B). Furthermore, a tight inverse relationship was found between the extent of FL-induced PSI photoinhibition and the maximum CO_2 assimilation rate (Fig. 7C), suggesting that the restriction of CO_2 fixation under drought stress accelerated FL-induced PSI photoinhibition. After the FL treatment, ETRII under high light significantly decreased in drought-stressed plants (Fig. 8). Concomitantly, Y(ND) significantly decreased and Y(NA) significantly increased (Fig. 8). These results indicated that the greater FL-induced PSI photoinhibition under drought stress significantly affected linear electron flow and PSI photoprotection under high light.

Discussion

In nature, FL usually occurs concomitantly with drought stress. However, the effects of drought stress on photosynthetic performances under FL are little known. We here for the first time examined the effects of drought stress on photosynthetic induction and PSI

306 photoinhibition under FL in tomato.

307

308 **Drought stress delayed photosynthetic induction under FL**

309 The response of A_N to a rapid change of light intensity plays an important role in
310 determining plant biomass under FL (Vialet-Chabrand, Matthews, Simkin, Raines & Lawson
311 2017; Slattery *et al.* 2018; Kimura *et al.* 2020; Yamori *et al.* 2020). Drought stress usually
312 decreases steady-state g_s, g_m, and A_N under constant high light (Warren *et al.* 2004; Huang *et*
313 *al.* 2013; Zivcak *et al.* 2013), but the effects of drought stress on the induction response of g_s,
314 g_m, and A_N under FL are not well known. Similar to previous studies, we found the maximum
315 g_s, g_m, and A_N under constant high light significantly declined in drought-stressed tomato
316 plants (Fig. 1). Moreover, drought stress largely affected the induction responses of g_s and g_m
317 after transition from low to high light and consequently delayed the induction response of A_N.
318 A_N in CK plants reached 80% of the maximum value approximately 2 min after transition
319 from 100 to 1500 μmol photons m^{-2} s^{-1} (Fig. 1). Such photosynthetic induction required 10
320 min in drought-stressed plants. Therefore, drought stress caused a larger loss of carbon gain
321 upon transition from low to high light in tomato. Similar to observations under drought stress,
322 tomato plants display relatively lower g_s under salt stress, and the decrease in g_s under salt
323 stress reduced plant biomass when grown under FL (Zhang, Kaiser, Marcelis, Yang & Li
324 2020). However, the underlying mechanisms of this response are not well known. Our present
325 study provided a possible explanation for why salt stress reduces plant biomass in tomato
326 plants grown under FL.

327 Recent studies indicate stomatal opening under FL could be affected by stomatal density
328 and area (Zhang *et al.* 2020; Sakoda *et al.* 2020). In the present study, the drought treatment
329 just lasted for 1 week, and we used mature leaves developed prior to the treatment period for
330 photosynthetic measurements. Therefore, the slower stomatal opening under drought stress
331 was independent of stomatal density and area and was likely caused by other factors such as
332 abscisic acid and gene regulation. Abscisic acid is upregulated under drought stress, which
333 could induce stomatal closure (Ramachandra & Viswanatha 2004; Harb, Krishnan,
334 Ambavaram & Pereira 2010; Kaiser, Morales, Harbinson, Heuvelink & Marcelis 2020).
335 Furthermore, the expression of *slow anion channel-associated 1* (*slac1*), *open stomata 1*

(*ost1*), and *proton ATPase translocation control 1* (*PATROL1*) play important roles in stomatal opening under FL (Kimura *et al.* 2020; Yamori *et al.* 2020). Drought stress might influence the expression of these target genes and thus affect the stomatal opening under FL.

Photosynthesis can be limited by g_s, g_m, and biochemical factors, but the relative photosynthetic limitations largely vary among species (Grassi & Magnani 2005; Carriquí *et al.* 2015; Xiong *et al.* 2018). We found that drought stress increased the diffusional limitation of A_N under FL, and the major limiting factor of photosynthesis was altered by drought stress (Fig. 3). In *Arabidopsis thaliana* and tobacco, CO_2 diffusional limitation was the major limiting factor of photosynthesis in the initial 10 min after transition from dark to light (Sakoda *et al.* 2021). By comparison, L_s, L_{mc} and L_b changed little after the transition from low to high light in the CK plants (Fig. 3). Therefore, the dynamic changes in relative limitations of A_N after the transition from low to high light differed from that after the transition from dark to high light. Due to decreased g_s and g_m under drought stress, C_c was lower in high-light phases under FL, and therefore photosynthesis under FL was strongly restricted by C_c (Fig. 2). Furthermore, after transition from low to high light, the C_c values in the CK plants were always higher than C_{trans} (Fig. 2), indicating that A_N was mainly limited by RuBP regeneration. By contrast, the C_c values under FL were always lower than C_{trans} under drought stress (Fig. 2), and hence A_N tended to be mainly limited by RuBP carboxylation. Therefore, the rate-limiting step for A_N during photosynthetic induction was influenced by drought stress.

Drought stress accelerated PSI photoinhibition under FL

A sudden increase in light intensity causes a rapid increase in PSII electron flow to PSI, whereas the full activation of CO_2 fixation requires more time (Lawson & Blatt 2014; Yamori *et al.* 2016). Therefore, the excited states in PSI cannot be immediately consumed by primary metabolism, leading to the accumulation of reducing power in PSI. The resulting PSI over-reduction promotes ROS formation in PSI and causes PSI photoinhibition (Yamori *et al.* 2016; Huang *et al.* 2019a). Under drought stress, lower g_s restricted CO_2 fixation and thus decreased the rate of NADPH production. Because the pool of NADPH is relatively small, drought stress will increase the NADPH/$NADP^+$ ratio when exposed to a sudden increase in

illumination. Under such conditions, electron flow from PSI to $NADP^+$ would be limited by the lack of $NADP^+$, suppressing the oxidation of PSI under FL (Grieco *et al.* 2020). Therefore, drought stress is hypothesized to accelerate PSI over-reduction under FL. Consistently, we found that PSI over-reduction under FL was aggravated under drought stress (Fig. 4). After a sudden increase in irradiance, tomato plants showed a transient PSI over-reduction in CK plants, indicating that the electrons transported to PSI could not be immediately consumed by downstream sinks. In angiosperms, outflows of electrons from PSI include two pathways: linear electron flow (LEF) (PSI to $NADP^+$) and the water-water cycle mediated by the Mehler reaction (Ilík *et al.* 2017; Shikanai & Yamamoto 2017). Recent studies have indicated that the water-water cycle can rapidly consume the excess reducing power in PSI and thus prevents a transient PSI over-reduction under FL (Huang *et al.* 2019b; Sun *et al.* 2020a). However, a transient PSI over-reduction under FL was clearly observed (Fig. 4C), indicating that the water-water cycle is negligible in tomato leaves. Therefore, the transient PSI over-reduction under FL is attributed to the limitation of LEF. Under drought stress, the restriction of CO_2 fixation caused LEF to be further restricted by the lack of $NADP^+$ and thus increased PSI over-reduction upon the transition from low to high light.

Once PSI is over-reduced under high light, the donation of electrons from PSI electron carriers to O_2 accelerates, aggravating the production of ROS within PSI (Takagi *et al.* 2016). Moreover, ROS produced within thylakoid membranes cannot be immediately scavenged by antioxidant systems (Takagi *et al.* 2016). Therefore, PSI over-reduction under high light easily causes PSI photoinhibition (Yamamoto & Shikanai 2019; Tan *et al.* 2021). Consistently, the stronger PSI over-reduction in FL accelerated PSI photoinhibition under drought stress (Fig. 7). Furthermore, the stronger PSI photoinhibition under drought stress led to decreased rETRII and Y(ND) and increased Y(NA), suggesting that light use efficiency and photoprotection were significantly affected by the PSI photoinhibition (Fig. 8). After photodamage, the recovery of PSI activity is a slow process that requires several days (Zhang & Scheller 2004; Zivcak *et al.* 2015). During the recovery period, the lower CO_2 assimilation rate impairs starch accumulation and plant growth (Lima-Melo, Gollan, Tikkanen, Silveira & Aro 2019). Therefore, when grown under FL, drought stress would decrease plant biomass partially owing to stronger PSI photoinhibition. In contrast to PSI, the PSII excitation pressure

under FL was slightly affected by drought stress (Fig. 5), which was consistent with previous studies reporting that PSII is tolerant to FL (Yamamoto & Shikanai 2019).

To protect PSI against photoinhibition under FL, angiosperms mainly use CEF to fine-tune the PSI redox state through regulation of ΔpH (Armbruster *et al.* 2017). Under low light, upon a low CEF activation, a relatively low ΔpH is formed to facilitate electron flow through Cyt b6/f and thus to maximize light use efficiency (Tikkanen & Aro 2014). Under high light, CEF is highly activated to generate a high ΔpH, which slows down the oxidation of plastoquinone and thus down-regulates the rate of electron transport toward PSI (Shikanai & Yamamoto 2017). When transitioning from low to high light, the full acidification of the thylakoid lumen requires dozens of seconds (Huang *et al.* 2019b; Yang, Zhang & Huang 2019b). Therefore, plants cannot generate sufficient ΔpH within the first seconds after an abrupt increase in irradiance. To avoid uncontrolled PSI over-reduction under FL, CEF rapidly activates to aid the formation of ΔpH (Kono *et al.* 2014; Yang *et al.* 2019a). In the present study, we found relative CEF activity in high-light phases of FL increased under drought stress (Fig. 6), suggesting that the relative contribution of CEF to ΔpH formation was enhanced in drought-stressed plants. Such up-regulation of CEF activity partially compensated for the restriction of CO_2 fixation and thus favored PSI photoprotection under FL.

Conclusions

We established that drought stress largely affects g_s and g_m after the transition from low to high light and thus delays photosynthetic induction under FL. Furthermore, restriction of CO_2 assimilation under drought stress accelerates PSI over-reduction under FL, which increases the susceptibility of PSI to photoinhibition. Therefore, drought stress strongly affects the photosynthetic dark and light reactions under FL. These findings provide insight into photosynthetic physiology under drought and FL.

References

Acevedo□Siaca L.G., Coe R., Wang Y., Kromdijk J., Quick W.P. & Long S.P. (2020)

Variation in photosynthetic induction between rice accessions and its potential for

426 improving productivity. *New Phytologist* **227**, 1097–1108.

427 Adachi S., Tanaka Y., Miyagi A., Kashima M., Tezuka A., Toya Y., … Yamori W. (2019)
428 High-yielding rice Takanari has superior photosynthetic response to a commercial rice
429 Koshihikari under fluctuating light. *Journal of Experimental Botany* **70**, 5287–5297.

430 Alboresi A., Storti M. & Morosinotto T. (2019) Balancing protection and efficiency in the
431 regulation of photosynthetic electron transport across plant evolution. *New Phytologist*
432 **221**, 105–109.

433 Allahverdiyeva Y., Suorsa M., Tikkanen M. & Aro E.M. (2015) Photoprotection of
434 photosystems in fluctuating light intensities. *Journal of Experimental Botany* **66**,
435 2427–2436.

436 Armbruster U., Correa Galvis V., Kunz H.H. & Strand D.D. (2017) The regulation of the
437 chloroplast proton motive force plays a key role for photosynthesis in fluctuating light.
438 *Current Opinion in Plant Biology* **37**, 56–62.

439 Baker N.R. (2004) Applications of chlorophyll fluorescence can improve crop production
440 strategies: an examination of future possibilities. *Journal of Experimental Botany* **55**,
441 1607–1621.

442 von Caemmerer S. & Evans J.R. (2015) Temperature responses of mesophyll conductance
443 differ greatly between species. *Plant, Cell and Environment* **38**, 629–637.

444 Carriquí M., Cabrera H.M., Conesa M., Coopman R.E., Douthe C., Gago J., … Flexas J.
445 (2015) Diffusional limitations explain the lower photosynthetic capacity of ferns as
446 compared with angiosperms in a common garden study. *Plant, Cell and Environment* **38**,
447 448–460.

448 Flexas J., Diaz-Espejo A., Gago J., Gallé A., Galmés J., Gulías J. & Medrano H. (2014)
449 Photosynthetic limitations in Mediterranean plants: A review. *Environmental and*
450 *Experimental Botany* **103**, 12–23.

451 Galmés J., Ochogavía J.M., Gago J., Roldán E.J., Cifre J. & Conesa M.À. (2013) Leaf
452 responses to drought stress in Mediterranean accessions of Solanum lycopersicum:
453 Anatomical adaptations in relation to gas exchange parameters. *Plant, Cell and*
454 *Environment* **36**, 920–935.

455 Genty B., Briantais J.-M. & Baker N.R. (1989) The relationship between the quantum yield of

456 photosynthetic electron transport and quenching of chlorophyll fluorescence. *Biochimica*
457 *et Biophysica Acta (BBA) - General Subjects* **990**, 87–92.
458 Gerotto C., Alboresi A., Meneghesso A., Jokel M., Suorsa M., Aro E.-M. & Morosinotto T.
459 (2016) Flavodiiron proteins act as safety valve for electrons in *Physcomitrella patens*.
460 *Proceedings of the National Academy of Sciences* **113**, 12322–12327.
461 Grassi G. & Magnani F. (2005) Stomatal, mesophyll conductance and biochemical limitations
462 to photosynthesis as affected by drought and leaf ontogeny in ash and oak trees. *Plant,*
463 *Cell and Environment* **28**, 834–849.
464 Grieco M., Roustan V., Dermendjiev G., Rantala S., Jain A., Leonardelli M., … Teige M.
465 (2020) Adjustment of photosynthetic activity to drought and fluctuating light in wheat.
466 *Plant, Cell & Environment* **43**, 1484–1500.
467 Harb A., Krishnan A., Ambavaram M.M.R. & Pereira A. (2010) Molecular and Physiological
468 Analysis of Drought Stress in Arabidopsis Reveals Early Responses Leading to
469 Acclimation in Plant Growth. *Plant Physiology* **154**, 1254–1271.
470 Harley P.C., Loreto F., Di Marco G. & Sharkey T.D. (1992) Theoretical considerations when
471 estimating the mesophyll conductance to CO2 flux by analysis of the response of
472 photosynthesis to CO2. *Plant Physiology* **98**, 1429–1436.
473 Huang W., Fu P.L., Jiang Y.J., Zhang J.L., Zhang S.B., Hu H. & Cao K.F. (2013) Differences
474 in the responses of photosystem I and photosystem II of three tree species Cleistanthus
475 sumatranus, Celtis philippensis and Pistacia weinmannifolia exposed to a prolonged
476 drought in a tropical limestone forest. *Tree Physiology*.
477 Huang W., Yang Y.-J. & Zhang S.-B. (2019a) Photoinhibition of photosystem I under
478 fluctuating light is linked to the insufficient ΔpH upon a sudden transition from low to
479 high light. *Environmental and Experimental Botany* **160**, 112–119.
480 Huang W., Yang Y.-J. & Zhang S.-B. (2019b) The role of water-water cycle in regulating the
481 redox state of photosystem I under fluctuating light. *Biochimica et Biophysica Acta*
482 *(BBA) - Bioenergetics* **1860**, 383–390.
483 Ilík P., Pavlovič A., Kouřil R., Alboresi A., Morosinotto T., Allahverdiyeva Y., … Shikanai T.
484 (2017) Alternative electron transport mediated by flavodiiron proteins is operational in
485 organisms from cyanobacteria up to gymnosperms. *New Phytologist* **214**, 967–972.

Kaiser E., Morales A., Harbinson J., Heuvelink E. & Marcelis L.F.M. (2020) High Stomatal Conductance in the Tomato Flacca Mutant Allows for Faster Photosynthetic Induction. *Frontiers in Plant Science* **11**, 1–12.

Kimura H., Hashimoto-Sugimoto M., Iba K., Terashima I. & Yamori W. (2020) Improved stomatal opening enhances photosynthetic rate and biomass production in fluctuating light. *Journal of Experimental Botany* **71**, 2339–2350.

Kono M., Noguchi K. & Terashima I. (2014) Roles of the cyclic electron flow around PSI (CEF-PSI) and O2-dependent alternative pathways in regulation of the photosynthetic electron flow in short-term fluctuating light in Arabidopsis thaliana. *Plant and Cell Physiology* **55**, 990–1004.

Krall J.P. & Edwards G.E. (1992) Relationship between photosystem II activity and CO2 fixation in leaves. *Physiologia Plantarum* **86**, 180–187.

Lawson T. & Blatt M.R. (2014) Stomatal Size, Speed, and Responsiveness Impact on Photosynthesis and Water Use Efficiency. *Plant Physiology* **164**, 1556–1570.

Lima-Melo Y., Gollan P.J., Tikkanen M., Silveira J.A.G. & Aro E.M. (2019) Consequences of photosystem-I damage and repair on photosynthesis and carbon use in Arabidopsis thaliana. *Plant Journal* **97**, 1061–1072.

Long S.P. & Bernacchi C.J. (2003) Gas exchange measurements, what can they tell us about the underlying limitations to photosynthesis? Procedures and sources of error. *Journal of Experimental Botany* **54**, 2393–2401.

Oukarroum A., Schansker G. & Strasser R.J. (2009) Drought stress effects on photosystem i content and photosystem II thermotolerance analyzed using Chl a fluorescence kinetics in barley varieties differing in their drought tolerance. *Physiologia Plantarum* **137**, 188–189.

Pearcy R.W. (1990) Sunflecks and photosynthesis in plant canopies. *Annual Review of Plant Physiology and Plant Molecular Biology* **41**, 421–453.

Qu M., Essemine J., Xu J., Ablat G., Perveen S., Wang H., … Zhu X. (2020) Alterations in stomatal response to fluctuating light increase biomass and yield of rice under drought conditions. *The Plant Journal* **104**, 1334–1347.

Ramachandra A. & Viswanatha K. (2004) Drought-induced responses of photosynthesis and

516 antioxidant metabolism in higher plants. **161**, 1189–1202.
517 Sakoda K., Yamori W., Groszmann M. & Evans J.R. (2021) Stomatal , mesophyll
518 conductance , and biochemical limitations to photosynthesis during induction Research
519 Article. 146–160.
520 Sakoda K., Yamori W., Shimada T., Sugano S.S., Hara-Nishimura I. & Tanaka Y. (2020)
521 Higher stomatal density improves photosynthetic induction and biomass production in
522 Arabidopsis under fluctuating light. *Frontiers in Plant Science* **11**, 1308.
523 Sejima T., Takagi D., Fukayama H., Makino A. & Miyake C. (2014) Repetitive short-pulse
524 light mainly inactivates photosystem i in sunflower leaves. *Plant and Cell Physiology* **55**,
525 1184–1193.
526 Shikanai T. & Yamamoto H. (2017) Contribution of cyclic and pseudo-cyclic electron
527 transport to the formation of proton motive force in chloroplasts. *Molecular Plant* **10**,
528 20–29.
529 Shimakawa G. & Miyake C. (2019) What quantity of photosystem I is optimum for safe
530 photosynthesis? *Plant Physiology* **179**, 1479–1485.
531 Slattery R.A., Walker B.J., Weber A.P.M. & Ort D.R. (2018) The impacts of fluctuating light
532 on crop performance. *Plant Physiology* **176**, 990–1003.
533 De Souza A.P., Wang Y., Orr D.J., Carmo□Silva E. & Long S.P. (2020) Photosynthesis
534 across African cassava germplasm is limited by Rubisco and mesophyll conductance at
535 steady state, but by stomatal conductance in fluctuating light. *New Phytologist* **225**,
536 2498–2512.
537 Sun H., Yang Y.-J. & Huang W. (2020a) The water-water cycle is more effective in
538 regulating redox state of photosystem I under fluctuating light than cyclic electron
539 transport. *Biochimica et Biophysica Acta (BBA) - Bioenergetics* **1861**, 148235.
540 Sun H., Zhang S.-B., Liu T. & Huang W. (2020b) Decreased photosystem II activity
541 facilitates acclimation to fluctuating light in the understory plant Paris polyphylla.
542 *Biochimica et Biophysica Acta (BBA) - Bioenergetics* **1861**, 148135.
543 Suorsa M., Jarvi S., Grieco M., Nurmi M., Pietrzykowska M., Rantala M., … Aro E.-M.
544 (2012) PROTON GRADIENT REGULATION5 is essential for proper acclimation of
545 Arabidopsis photosystem I to naturally and artificially fluctuating light conditions. *The*

546 *Plant Cell* **24**, 2934–2948.

547 Takagi D., Takumi S., Hashiguchi M., Sejima T. & Miyake C. (2016) Superoxide and singlet
548 oxygen produced within the thylakoid membranes both cause photosystem I
549 photoinhibition. *Plant Physiology* **171**, 1626–1634.

550 Tan S.-L., Huang J.-L., Zhang F.-P., Zhang S.-B. & Huang W. (2021) Photosystem I
551 photoinhibition induced by fluctuating light depends on background low light irradiance.
552 *Environmental and Experimental Botany* **181**, 104298.

553 Tanaka Y., Adachi S. & Yamori W. (2019) Natural genetic variation of the photosynthetic
554 induction response to fluctuating light environment. *Current Opinion in Plant Biology*
555 **49**, 52–59.

556 Tazoe Y., Ishikawa N., Shikanai T., Ishiyama K., Takagi D., Makino A., … Endo T. (2020)
557 Overproduction of PGR5 enhances the electron sink downstream of photosystem I in a
558 C 4 plant, Flaveria bidentis. *The Plant Journal* **103**, 814–823.

559 Tikkanen M. & Aro E.M. (2014) Integrative regulatory network of plant thylakoid energy
560 transduction. *Trends in Plant Science* **19**, 10–17.

561 Vialet-Chabrand S., Matthews J.S.A., Simkin A.J., Raines C.A. & Lawson T. (2017)
562 Importance of Fluctuations in Light on Plant Photosynthetic Acclimation. *Plant*
563 *Physiology* **173**, 2163–2179.

564 Wada S., Yamamoto H., Suzuki Y., Yamori W., Shikanai T. & Makino A. (2018) Flavodiiron
565 protein substitutes for cyclic electron flow without competing CO2 assimilation in rice.
566 *Plant Physiology* **176**, 1509–1518.

567 Warren C.., Livingston N.J. & Turpin D.H. (2004) Water stress decreases the transfer
568 conductance of Douglas-fir (Pseudotsuga menziesii) seedlings. *Tree physiology* **24**,
569 971–979.

570 Warren C.R. & Dreyer E. (2006) Temperature response of photosynthesis and internal
571 conductance to CO2: Results from two independent approaches. *Journal of*
572 *Experimental Botany* **57**, 3057–3067.

573 Xiong D., Douthe C. & Flexas J. (2018) Differential coordination of stomatal conductance,
574 mesophyll conductance, and leaf hydraulic conductance in response to changing light
575 across species. *Plant, Cell & Environment* **41**, 436–450.

576 Yamamoto H. & Shikanai T. (2019) PGR5-dependent cyclic electron flow protects
577 photosystem I under fluctuating light at donor and acceptor sides. *Plant Physiology* **179**,
578 588–600.
579 Yamori W., Evans J.R. & Von Caemmerer S. (2010a) Effects of growth and measurement
580 light intensities on temperature dependence of CO2 assimilation rate in tobacco leaves.
581 *Plant, Cell and Environment* **33**, 332–343.
582 Yamori W., Kusumi K., Iba K. & Terashima I. (2020) Increased stomatal conductance
583 induces rapid changes to photosynthetic rate in response to naturally fluctuating light
584 conditions in rice. *Plant, Cell & Environment* **43**, 1230–1240.
585 Yamori W., Makino A. & Shikanai T. (2016) A physiological role of cyclic electron transport
586 around photosystem I in sustaining photosynthesis under fluctuating light in rice.
587 *Scientific reports* **6**, 20147.
588 Yamori W., Nagai T. & Makino A. (2011) The rate-limiting step for CO2 assimilation at
589 different temperatures is influenced by the leaf nitrogen content in several C3 crop
590 species. *Plant, Cell and Environment* **34**, 764–777.
591 Yamori W., Noguchi K., Hikosaka K. & Terashima I. (2010b) Phenotypic plasticity in
592 photosynthetic temperature acclimation among crop species with different cold
593 tolerances. *Plant Physiology* **152**, 388–399.
594 Yang Y.-J., Ding X.-X. & Huang W. (2019a) Stimulation of cyclic electron flow around
595 photosystem I upon a sudden transition from low to high light in two angiosperms
596 Arabidopsis thaliana and Bletilla striata. *Plant Science* **287**, 110166.
597 Yang Y.-J., Zhang S.-B. & Huang W. (2019b) Photosynthetic regulation under fluctuating
598 light in young and mature leaves of the CAM plant Bryophyllum pinnatum. *Biochimica*
599 *et Biophysica Acta (BBA) - Bioenergetics* **1860**, 469–477.
600 Zhang S. & Scheller H.V. (2004) Photoinhibition of photosystem I at chilling temperature and
601 subsequent recovery in Arabidopsis thaliana. *Plant and Cell Physiology* **45**, 1595–1602.
602 Zhang Y., Kaiser E., Marcelis L.F.M., Yang Q. & Li T. (2020) Salt stress and fluctuating
603 light have separate effects on photosynthetic acclimation, but interactively affect
604 biomass. *Plant, Cell & Environment* **43**, 2192–2206.
605 Zivcak M., Brestic M., Balatova Z., Drevenakova P., Olsovska K., Kalaji H.M., …

606 Allakhverdiev S.I. (2013) Photosynthetic electron transport and specific photoprotective
607 responses in wheat leaves under drought stress. *Photosynthesis Research* **117**, 529–546.
608 Zivcak M., Brestic M., Kunderlikova K., Sytar O. & Allakhverdiev S.I. (2015) Repetitive
609 light pulse-induced photoinhibition of photosystem I severely affects CO2 assimilation
610 and photoprotection in wheat leaves. *Photosynthesis Research* **126**, 449–463.
611
612

613 **Figure legends**

614 **Figure 1.** The effects of drought stress on photosynthetic induction after transition from low
615 to high light. Time course of net CO_2 assimilation (A_N; A and B), stomatal conductance (g_s; C
616 and D) and mesophyll conductance (g_m; E and F) after transition from 100 to 1500 μmol
617 photons m^{-2} s^{-1}. Before this measurement, leaves were adapted to low irradiance (100 μmol
618 photons m^{-2} s^{-1}) for 5 min. A_N, g_s and g_m were normalized against the maximum values after
619 photosynthetic induction for 30 min. Values are means ± SE of five independent experiments
620 (n = 5).

621

622 **Figure 2.** Effects of drought stress on the time course of intercellular CO_2 concentration (C_i;
623 A) and chloroplast CO_2 concentration (C_c; B), and the relationship between C_c and A_N after
624 transition from low to high light. Red and grey dotted lines represent the values of C_{trans} (the
625 chloroplast CO_2 concentration at which the limitation to A_N transitioned from RuBP
626 carboxylation to RuBP regeneration) in CK and drought stressed plants, respectively. The
627 experimental design was the same as described in Figure 1. Values are means ± SE of five
628 independent experiments (n = 5).

629

630 **Figure 3.** Effects of drought stress on the quantitative analysis of stomatal limitation (L_s),
631 mesophyll conductance limitation (L_{mc}) and biochemical limitation (L_b) after transition from
632 low to high light. The experimental design was the same as described in Figure 1. Values are
633 means ± SE of five independent experiments (n = 5).

634

635 **Figure 4.** Effects of drought stress on photosystem I parameter under fluctuating light
636 alternating between 59 μmol photons m^{-2} s^{-1} (2 min) and 1455 μmol photons m^{-2} s^{-1} (1 min).
637 Y(I), the quantum yield of PSI photochemistry; Y(ND), the quantum yield of PSI
638 non-photochemical energy dissipation due to donor side limitation; Y(NA), the quantum yield
639 of PSI non-photochemical energy dissipation due to acceptor side limitation. Values are
640 means ± SE of five independent experiments (n = 5).

641

642

643 **Figure 5.** Effects of drought stress on photosystem II parameter under fluctuating light
644 alternating between 59 μmol photons m^{-2} s^{-1} (2 min) and 1455 μmol photons m^{-2} s^{-1} (1 min).
645 Y(II), the quantum yield of PSII photochemistry; NPQ, non-photochemical quenching in PSII;
646 Y(NO), the quantum yield of non-regulatory energy dissipation in PSII. Values are means ±
647 SE of five independent experiments (n = 5).
648
649 **Figure 6.** Effects of drought stress on photosynthetic electron transport rate under fluctuating
650 light alternating between 59 μmol photons m^{-2} s^{-1} (2 min) and 1455 μmol photons m^{-2} s^{-1} (1
651 min). rETRI, the relative electron transport rate through PSI; rETRII, the relative electron
652 transport rate through PSII; Relative CEF/LEF, the relative cyclic and linear electron flow
653 ratio. Values are means ± SE of five independent experiments (n = 5).
654
655 **Figure 7.** Effects of drought stress on PSI photoinhibition after fluctuating light treatment. (A)
656 The extent of PSI photoinhibition was measured by the decrease in Pm; (B) The relationship
657 between PSI over-reduction within the first 30 s after transition from low to high light
658 [average $Y(NA)_{30s}$] and PSI photoinhibition; (C) The relationship between the maximum CO_2
659 assimilation rate during photosynthetic induction (A_{max}) and PSI photoinhibition. Values are
660 means ± SE of five independent experiments (n = 5). Asterisk indicates a significant different
661 between the CK-plants and drought-stressed plants.
662
663 **Figure 8.** Effects of drought stress on values of rETR, Y(ND) and Y(NA) 1455 μmol photons
664 m^{-2} s^{-1} after fluctuating light treatment. Values are means ± SE of five independent
665 experiments (n = 5). Asterisk indicates a significant different between the CK-plants and
666 drought-stressed plants.
667

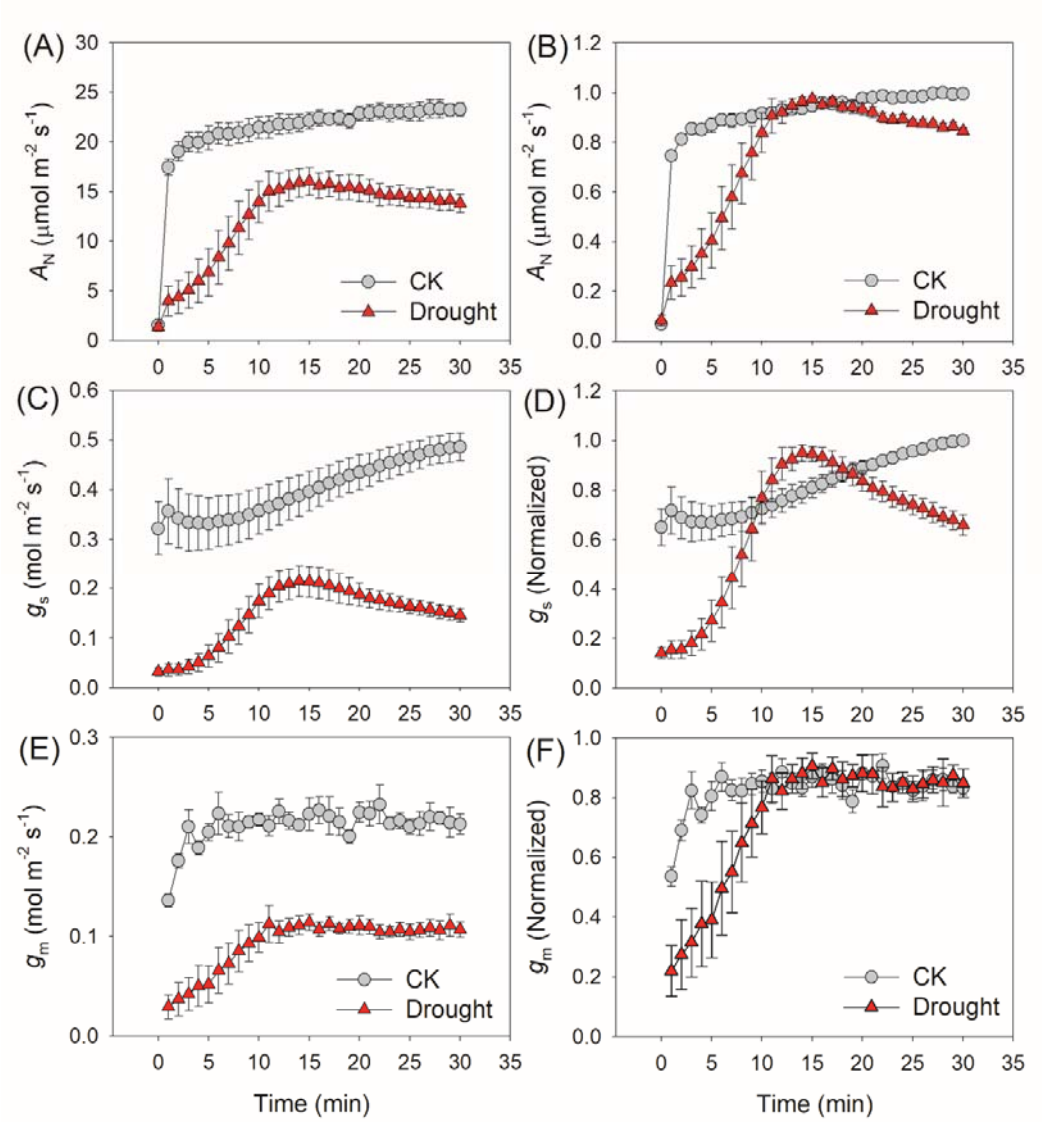

Figure 1. The effects of drought stress on photosynthetic induction after transition from low to high light. Time course of net CO_2 assimilation (A_N; A and B), stomatal conductance (g_s; C and D) and mesophyll conductance (g_m; E and F) after transition from 100 to 1500 μmol photons m^{-2} s^{-1}. Before this measurement, leaves were adapted to low irradiance (100 μmol photons m^{-2} s^{-1}) for 5 min. A_N, g_s and g_m were normalized against the maximum values after photosynthetic induction for 30 min. Values are means ± SE of five independent experiments (n = 5).

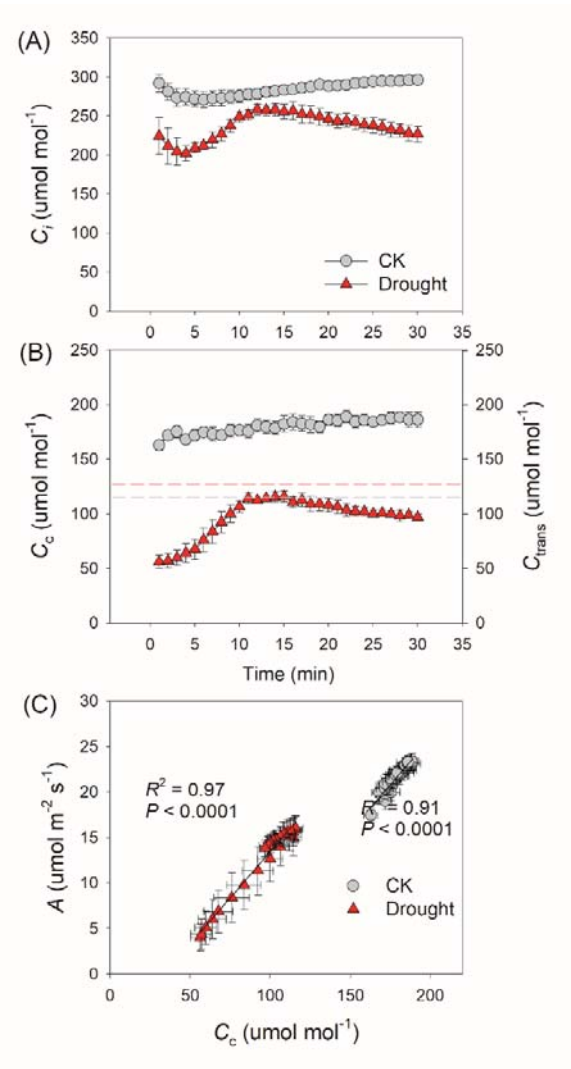

Figure 2. Effects of drought stress on the time course of intercellular CO_2 concentration (C_i; A) and chloroplast CO_2 concentration (C_c; B), and the relationship between C_c and A_N after transition from low to high light. Red and grey dotted lines represent the values of C_{trans} (the chloroplast CO_2 concentration at which the limitation to A_N transitioned from RuBP carboxylation to RuBP regeneration) in CK and drought stressed plants, respectively. The experimental design was the same as described in Figure 1. Values are means ± SE of five independent experiments (n = 5).

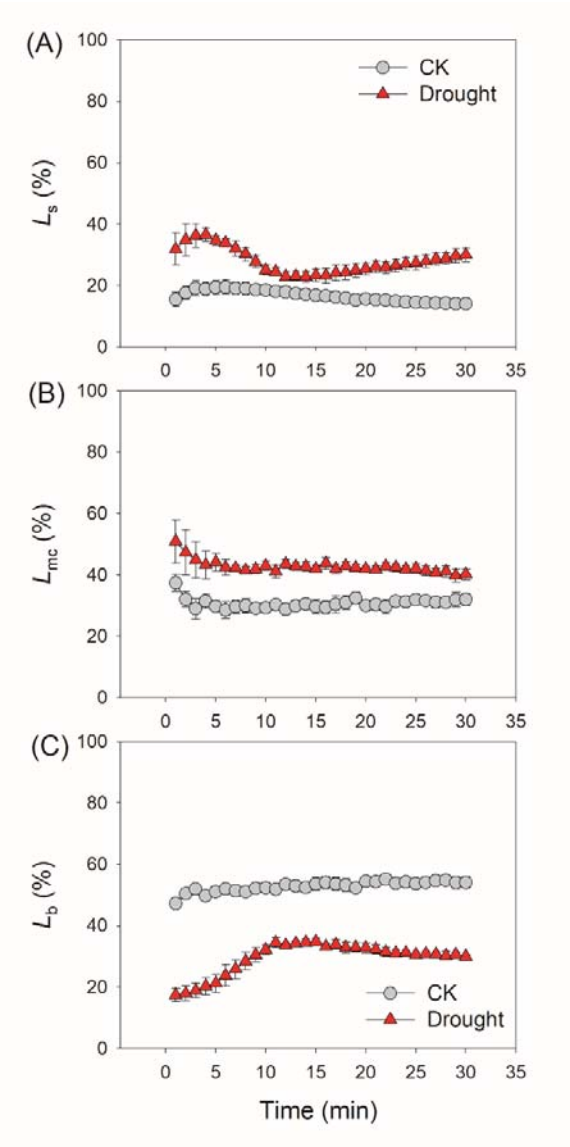

Figure 3. Effects of drought stress on the quantitative analysis of stomatal limitation (L_s), mesophyll conductance limitation (L_{mc}) and biochemical limitation (L_b) after transition from low to high light. The experimental design was the same as described in Figure 1. Values are means ± SE of five independent experiments (n = 5).

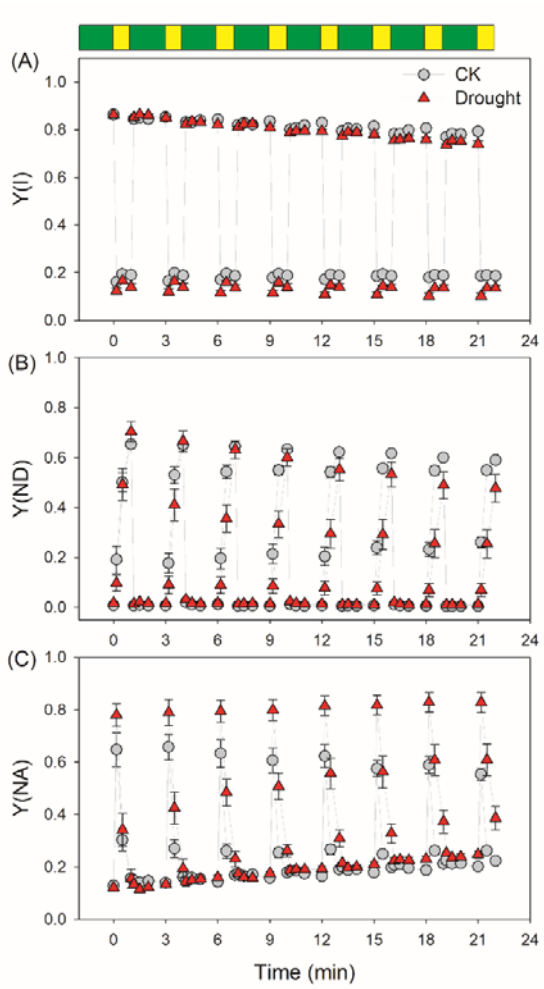

Figure 4. Effects of drought stress on photosystem I parameter under fluctuating light alternating between 59 μmol photons m^{-2} s^{-1} (2 min) and 1455 μmol photons m^{-2} s^{-1} (1 min). Y(I), the quantum yield of PSI photochemistry; Y(ND), the quantum yield of PSI non-photochemical energy dissipation due to donor side limitation; Y(NA), the quantum yield of PSI non-photochemical energy dissipation due to acceptor side limitation. Values are means ± SE of five independent experiments (n = 5).

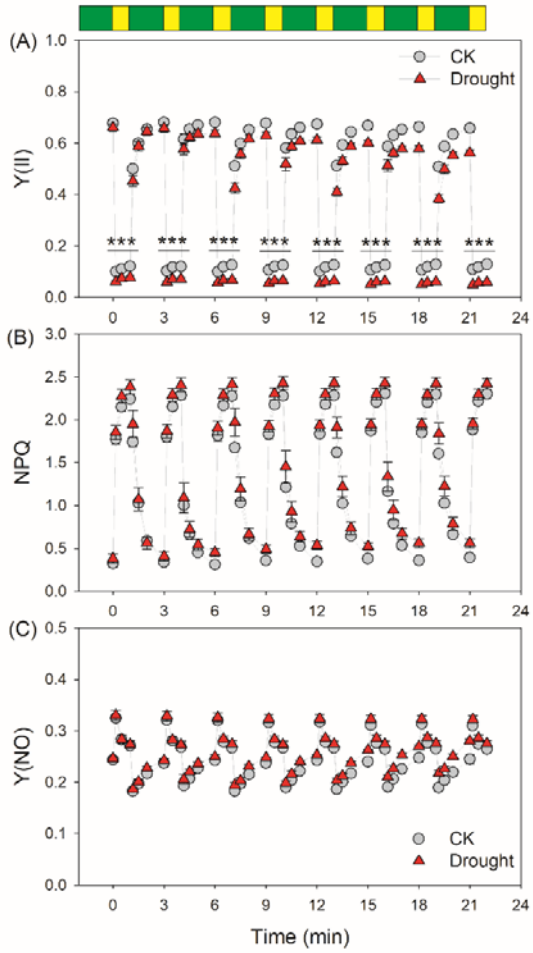

Figure 5. Effects of drought stress on photosystem II parameter under fluctuating light alternating between 59 μmol photons m^{-2} s^{-1} (2 min) and 1455 μmol photons m^{-2} s^{-1} (1 min). Y(II), the quantum yield of PSII photochemistry; NPQ, non-photochemical quenching in PSII; Y(NO), the quantum yield of non-regulatory energy dissipation in PSII. Values are means ± SE of five independent experiments (n = 5).

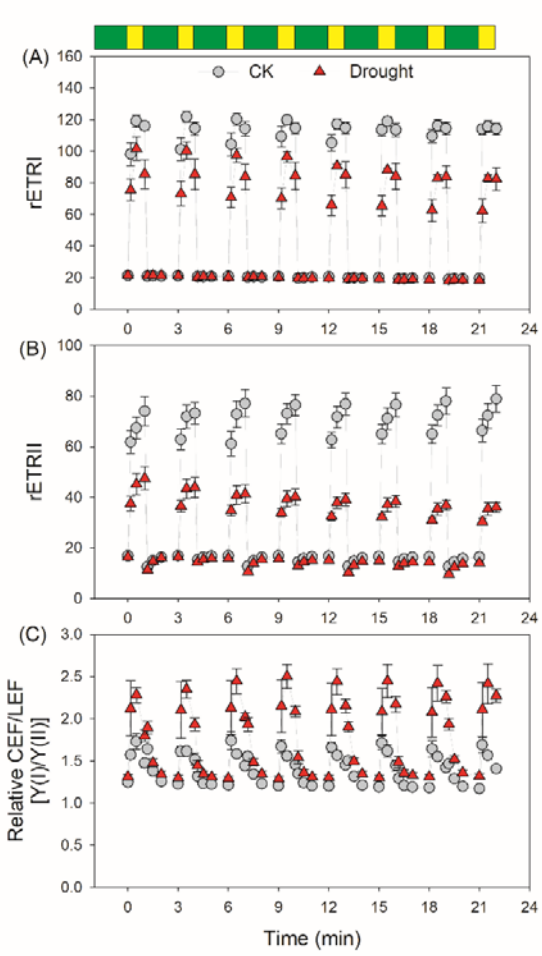

Figure 6. Effects of drought stress on photosynthetic electron transport rate under fluctuating light alternating between 59 μmol photons m^{-2} s^{-1} (2 min) and 1455 μmol photons m^{-2} s^{-1} (1 min). rETRI, the relative electron transport rate through PSI; rETRII, the relative electron transport rate through PSII; Relative CEF/LEF, the relative cyclic and linear electron flow ratio. Values are means ± SE of five independent experiments (n = 5).

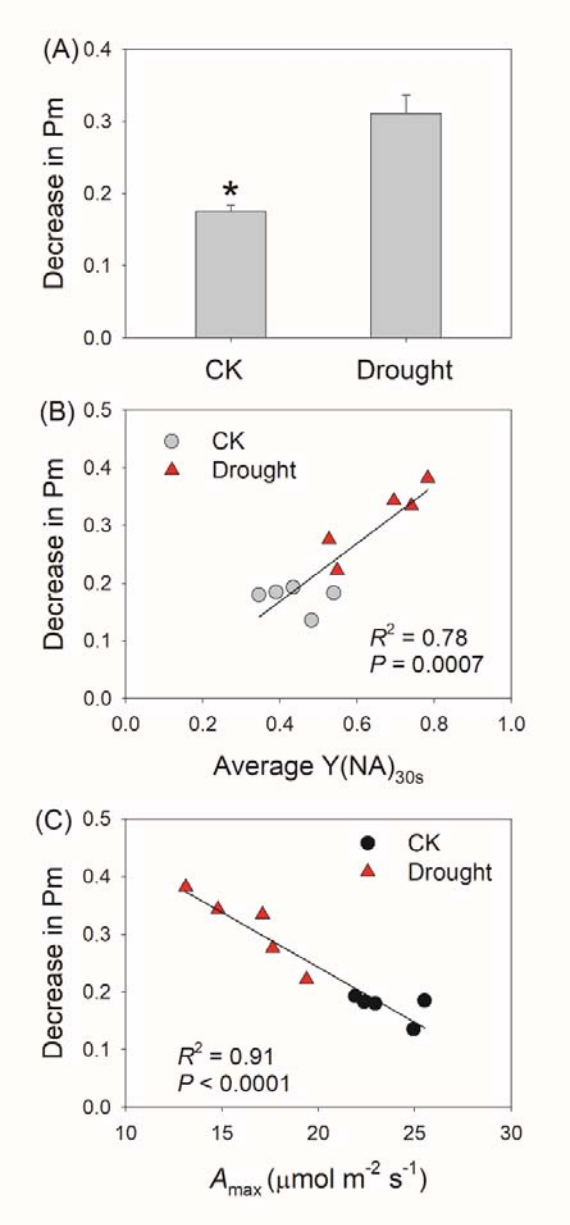

Figure 7. Effects of drought stress on PSI photoinhibition after fluctuating light treatment. (A) The extent of PSI photoinhibition was measured by the decrease in Pm; (B) The relationship between PSI over-reduction within the first 30 s after transition from low to high light [average $Y(NA)_{30s}$] and PSI photoinhibition; (C) The relationship between the maximum CO_2 assimilation rate during photosynthetic induction (A_{max}) and PSI photoinhibition. Values are means ± SE of five independent experiments (n = 5). Asterisk indicates a significant different between the CK-plants and drought-stressed plants.

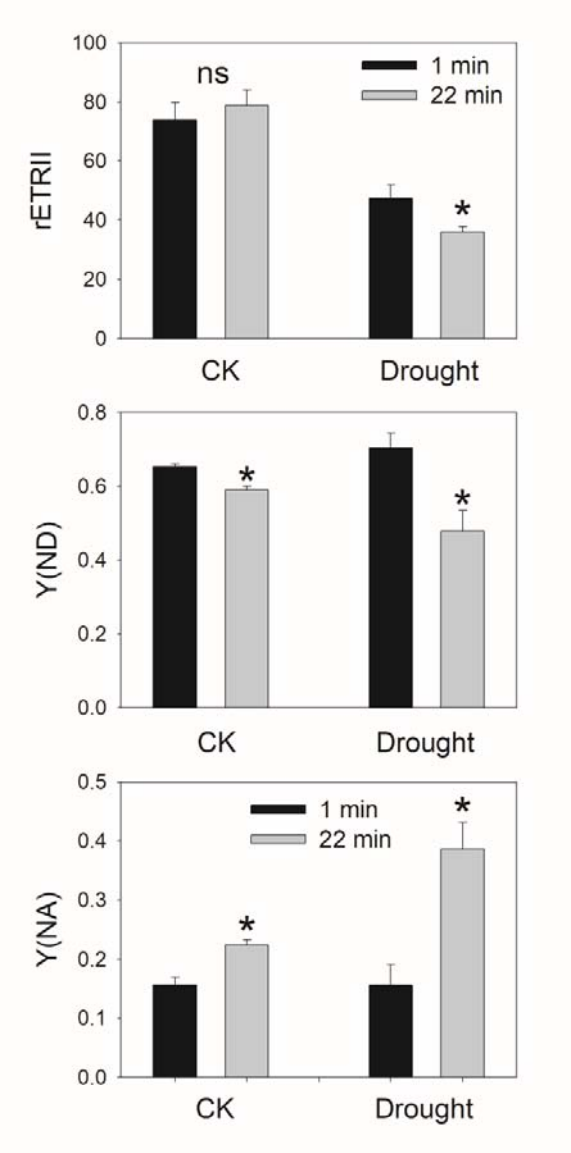

Figure 8. Effects of drought stress on values of rETR, Y(ND) and Y(NA) 1455 μmol photons m^{-2} s^{-1} after fluctuating light treatment. Values are means ± SE of five independent experiments (n = 5). Asterisk indicates a significant different between the CK-plants and drought-stressed plants.